

# Optical Engineering

OpticalEngineering.SPIEDigitalLibrary.org

## **Handy method to estimate uncertainty of temperature measurement by infrared thermography**

Pablo Rodrigues Muniz  
Ricardo de Araújo Kalid  
Shirley P. N. Cani  
Robson da Silva Magalhães

# Handy method to estimate uncertainty of temperature measurement by infrared thermography

Pablo Rodrigues Muniz,<sup>a,b,\*</sup> Ricardo de Araújo Kalid,<sup>b</sup> Shirley P. N. Cani,<sup>a</sup> and Robson da Silva Magalhães<sup>b</sup>

<sup>a</sup>Instituto Federal do Espírito Santo (IFES), Campus Vitória, Eletrotechnical Department, Vitória Avenue, 1729. Vitória / ES, 29040-780 Brazil

<sup>b</sup>Universidade Federal da Bahia (UFBA), Post-Graduate Program in Industrial Engineering, Aristides Novis St, 2. Salvador / BA, 40210-630 Brazil

**Abstract.** Temperature measurement by infrared thermography is a technique that is widely used in predictive maintenance to detect faults. The uncertainty involved in measuring temperature by thermography is not only due to the imager, but also due to the measurements and estimates made by the user: emissivity of the inspected object, distance, temperature, and relative humidity of the propagation medium, temperature of objects located in the ambient, and the imager itself. This measurement uncertainty should be available for the thermographer to be able to make a more accurate diagnosis. The methods available in the literature to estimate the uncertainty of measured temperature usually require information nonaccessible to the regular thermographer. This paper proposes a method for calculating the uncertainty of temperature that requires only data available to the thermographer. This method is useful under usual conditions in predictive maintenance—short distance (7.5 to 14  $\mu\text{m}$ ) thermal imagers, no fog or rain, among others. It provides results similar to methods that use models that are not available or reserved by the manufacturers of imagers. The results indicate that not all sources of uncertainty are relevant in measurement uncertainty. However, the total uncertainty can be so high that it may lead to misdiagnosis. © The Authors. Published by SPIE under a Creative Commons Attribution 3.0 Unported License. Distribution or reproduction of this work in whole or in part requires full attribution of the original publication, including its DOI. [DOI: [10.1117/1.OE.53.7.074101](https://doi.org/10.1117/1.OE.53.7.074101)]

Keywords: infrared thermography; measurement uncertainty; predictive maintenance.

Paper 140655 received Apr. 22, 2014; revised manuscript received Jun. 11, 2014; accepted for publication Jun. 13, 2014; published online Jul. 4, 2014.

## 1 Introduction

Temperature measurement by infrared thermography is liable to several sources of uncertainty both internal and external to the imager.<sup>1,2</sup> These uncertainties somehow combine and propagate to affect the result of the measurement system, i.e., the measured temperature of the inspected object. In other words, a temperature measured by thermography has an uncertainty, which is a combination of all sources of uncertainties.<sup>3</sup>

Internal sources of uncertainty are well understood and their influence is presented in a condensed way by manufacturers as the performance characteristics of the imager, for example, in the expected range of uncertainty for the measurements, such as thermal sensitivity and others.<sup>4</sup> Alternatively, these internal sources of uncertainty can be estimated from the calibration certificate.<sup>5</sup> Proper calibration methods can provide the total measurement uncertainty of the thermal imager due to its several internal sources of uncertainty.<sup>6</sup>

Temperature measurement by thermography also involves other instruments besides the thermal imager, such as the thermometer, hygrometer, and measuring tape (or a laser distance meter). The atmospheric temperature (propagation medium temperature), relative humidity, the distance between the imager and the inspected object, and the temperature of objects located in the ambient (ambient temperature) also have to be measured. The thermographer estimates the emissivity of the inspected object. These measurements are considered here as sources of uncertainty outside the imager. The works presented in Refs. 7 and 8 present a method for

calculating the uncertainty of temperature measurement considering the uncertainties of transmittance of the propagating medium, of the object's emissivity, and of the thermal imager. However, some information is not generally available to the thermographer. This includes (1) the transmittance of the propagating medium and its associated uncertainty and (2) the mathematical model, i.e., the spectral sensitivity of the thermal imager employed. This information is generally not available.<sup>9,10</sup>

Thus, the works presented in Refs. 7 and 8 describe a method for calculating the measurement uncertainty associated with the temperature measured by thermography. However, they are not useful as they require some information generally not available in the data sheet or in the user's manuals of the measurement instruments.

The search for methods for calculating the uncertainty of the temperature measurement by thermography has encouraged us to contact manufacturers of thermal imagers. We found that the thermal processing image and analysis software provided by the manufacturers does not calculate the measurement uncertainty, in spite of "when reporting the result of a measurement of a physical quantity, it is obligatory that some quantitative indication of the quality of the result be given so that those who use it can assess its reliability."<sup>3</sup> It would be appropriate for such software to estimate the uncertainty of the temperature measurement, but the determination of the uncertainty due to sources outside the imager is the user's responsibility.<sup>6</sup>

In general, the calculation models for uncertainty are reserved by the manufacturers.<sup>8</sup> Occasionally, only upon request, the manufacturer will provide the output data (uncertainty associated with the temperature measurement by thermography) from the input data (uncertainty of measurement

\*Address all correspondence to: Pablo R. Muniz, E-mail: [pablorm@ifes.edu.br](mailto:pablorm@ifes.edu.br)

instruments) informed by the client/customer.<sup>9,10</sup> However, the calculation method is not available.

The work presented in Ref. 11 suggests a laboratorial procedure to determine the function that relates the internal camera signal to the temperature of the inspected object. Unfortunately, this procedure is not practical for the regular thermographer because the resources needed are not common in service shops and because thermal imagers may use different internal calibration models.<sup>11</sup>

In addition to the recommendation that all measurements should be accompanied by their associated uncertainty,<sup>3</sup> the estimation of measurement temperature uncertainty helps the thermographer to make more accurate diagnoses. For instance, in electrical maintenance, the criteria of temperature difference indicative of faults is  $\sim 5^{\circ}\text{C}$ ,<sup>12-15</sup> a value for which the measurement uncertainty should be a maximum of 1 to  $2^{\circ}\text{C}$  (approximately one third of the tolerance of the measurement process).<sup>16,17</sup>

This paper presents a calculation method to estimate the uncertainty of temperature measurement by infrared thermography in predictive maintenance due to the uncertainties of the instruments used and measurements taken by the thermographer from data usually available to him/her. These are the distance between the inspected object and the thermal imager, the atmospheric temperature and the relative humidity, the emissivity of the object, the temperature of the objects located in the ambient, and the imager itself. It is assumed that the thermographer performs the thermographic inspection according to the recommendations of the thermal imager manufacturer, respecting the angle of view limits, the minimum inspected object dimensions, etc.

In addition to estimating measurement uncertainty, we estimate the contribution from each source of uncertainty for the final uncertainty measurement so as to enable the thermographer to analyze and prioritize investment to improve the quality of temperature measurement.

## 2 Calculation

As mathematical models of thermal imagers that correlate the spectral excittance received and the temperature of the inspected object are not available, we used general phenomenological and empirical models available in the literature. Of course, these models do not consider the aberrations and nonlinearities of each imager;<sup>1</sup> however, they provide a “quantitative indication of the quality of the outcome”<sup>3</sup> of the measured temperature, which nowadays is not made available by the manufacturers of thermal imagers and software developers.

### 2.1 Quantities Involved in Temperature Measurement by Thermography

In a survey of four Internet sites of manufacturers of imagers, we found that the imagers recommended for predictive maintenance operate approximately in the range of 7.5 to  $14\ \mu\text{m}$ .<sup>18-21</sup> This paper, therefore, focuses on this wavelength range. For this range transmittance, atmospheric absorption, which is the predominant factor for atmospheric attenuation, is virtually independent of the wavelength.<sup>22</sup>

In the operating wavelength range of thermal imagers used in predictive maintenance,<sup>2</sup> 7.5 to  $14\ \mu\text{m}$ , the method available in Ref. 22 can be used to calculate atmospheric transmittance.

The calculating method available in Ref. 22 considers that concentrations of absorbers like nitrous oxide, carbon monoxide, oxygen, methane, and nitrogen can be considered constant and their contributions irrelevant to practical problems of thermography. The concentration of water vapor varies widely according to the location and climate and is relevant in calculation of attenuation. The concentration of carbon dioxide ( $\text{CO}_2$ ) can be considered almost constant at  $\sim 0.032\%$  and, in principle, it should be considered in the calculation of atmospheric attenuation. However, when considering the works published in Refs. 23 and 24, it is noted that the atmospheric transmittance due to the concentration of  $\text{CO}_2$  is almost unitary in the range of 7.5 to  $14\ \mu\text{m}$  for propagation distances  $< 200\ \text{m}$ , common in thermography applied to predictive maintenance. Thus, the calculation of atmospheric attenuation is summarized in calculating the attenuation due to water molecules existing in the propagation path. Thus, the method consists in calculating the atmospheric internal transmittance, as only their absorption effect is relevant.<sup>2</sup>

Considering the uncertainty sources of interest, as previously defined in Sec. 1 (the distance between the inspected object and the imager, atmospheric temperature, relative humidity, emissivity of the object, ambient temperature, and the thermal imager), the calculation method is presented as a flow chart in Fig. 1. The definition of the calculation methods and calculation results provide the basis for calculating the propagation of uncertainty from these sources to the measured temperature for the inspected object.

Absolute humidity is a characteristic of the propagation medium that is not readily available. However, it can be

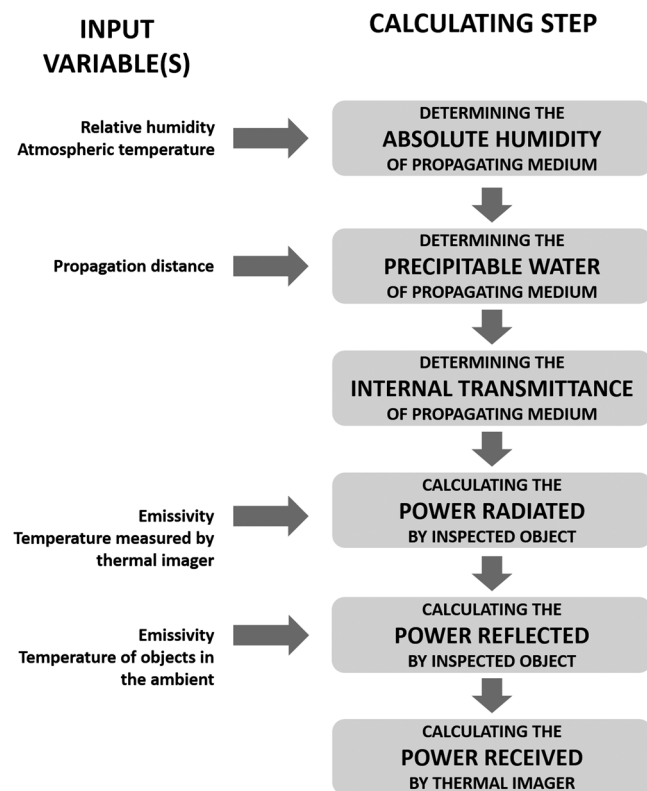


Fig. 1 Method for calculating the quantities involved in infrared thermography.

calculated from the relative humidity and atmospheric temperature, quantities easily measurable by the thermographer, with Eq. (1)<sup>25</sup>

$$\rho = 1322.8 \cdot \frac{UR}{T_{ATM}} \cdot \exp \left[ \frac{25.22 \cdot (T_{ATM} - 273.16)}{T_{ATM}} - 5.31 \cdot \ln \left( \frac{T_{ATM}}{273.16} \right) \right], \quad (1)$$

where  $UR$  is the relative humidity of the propagation medium (dimensionless),  $T_{ATM}$  is the propagation medium temperature (unit: K); and  $\rho$  is the absolute humidity of air in the propagation path (unit:  $\text{g} \cdot \text{m}^{-3}$ ).

Once the absolute humidity is obtained, the amount of precipitable water in the propagation medium is calculated according to Eq. (2)<sup>25,26</sup>

$$\delta = 10^{-3} \cdot \rho \cdot z, \quad (2)$$

where  $\delta$  is the amount of precipitable water (unit: mm) and  $z$  is the length of the propagation path of the electromagnetic field from the object to the thermal imager (unit: m).

The transmittance of the propagating medium can be obtained by consulting the Passman and Larmore tables available in Refs. 22, 23, and 27. The required input data are the amount of precipitable water and the wavelength of interest. It is noteworthy that within the wavelength range of interest in predictive maintenance (7.5 to 14  $\mu\text{m}$ ), atmospheric attenuation may be considered independent of wavelength<sup>22</sup> and dependent only on the amount of water precipitable, as the influence of  $\text{CO}_2$  is considered irrelevant. Therefore, the transmittance can be computed from three ascertainable variables: distance between the imager and the inspected object, temperature, and relative humidity of the propagation medium.

The total radiation received by the thermal imager is made up of radiation from the inspected object, radiation from the other surfaces located in the environment and reflected on the inspected surface, and radiation from the column of air between the inspected surface and the thermal imager.<sup>28</sup>

For short distances, the radiation from the column of air is negligible.<sup>28</sup> As a result, the radiation that will achieve the thermal imager comes only from the inspected object: radiation emitted by itself and reflected from the other surfaces in the ambient. Not considering the atmospheric transmittance, it can be computed as Eq. (3)<sup>28</sup>

$$R(\lambda, T_{ob}, T_A) = K \cdot [\varepsilon_\lambda \cdot I(\lambda, T_{ob}) + (1 - \varepsilon_\lambda) \cdot I(\lambda, T_A)], \quad (3)$$

where  $R(\lambda, T_{ob}, T_A)$  is the response of the thermal imager;  $T_{ob}$  is the absolute temperature of the object under inspection (unit: K);  $T_A$  is the absolute temperature of the objects in the ambient (unit: K);  $K$  is a coefficient, which is a function of the thermal imager, and includes some constants present in Planck's law;  $\varepsilon_\lambda$  is the inspected object's spectral emissivity (dimensionless);  $I(\lambda, T_X)$  represents the Planck radiation equation integrated over the spectral band of the imager, at temperature  $T_X$ ; and  $\lambda$  is the wavelength analyzed (unit:  $\mu\text{m}$ ).<sup>28</sup>

The transmittance, in this case due to atmospheric absorption, is considered in Eq. (4)<sup>1,25</sup>

$$R[z] = \frac{R[0]}{\tau[z]}, \quad (4)$$

where  $R[z]$  is the power from the inspected object at a distance  $z$  from the imager,  $R[0]$  is the radiation received by the imager, and  $\tau[z]$  is the transmittance of the medium between the imager and the object (dimensionless).

For wavelengths from 7.5 to 14  $\mu\text{m}$  and temperatures  $<500$  K, a common situation in predictive maintenance, the function  $I(\lambda, T_X)$ , can be expressed as Eq. (5)<sup>28</sup>

$$I(\lambda, T_X) = \frac{1}{\lambda^4 \cdot \exp[1.44 \times 10^4 / (\lambda \cdot T_X)]}. \quad (5)$$

As the user informs all the parameters on the right side of Eq. (3), the coefficient  $K$  is considered hypothetically unitary and a hypothetical response of the thermal imager is calculated. As a multiplying factor, this coefficient does not influence the calculation.

Emissivity will be considered constant in the wavelength range and not temperature dependent over the measuring range.<sup>11</sup> The nondependence of temperature considers that no significant superficial changes, which could affect its emissivity, occur to the inspected object.<sup>11</sup>

## 2.2 Uncertainty of the Temperature Measured by Thermography

To calculate the uncertainty output, that is, the uncertainty of the temperature measured, a knowledge of the mathematical models involved in this process is required. With these models, one can apply the law of propagation of uncertainty from the inputs to the output. If the input variables are uncorrelated, Eq. (6) is applied. All variables are considered uncorrelated because this consideration yields negligible errors.<sup>10,11</sup>

$$u_c^2(y) = \sum_{i=1}^N \left[ \frac{\partial f}{\partial x_i} \right]^2 \cdot u^2(x_i), \quad (6)$$

where  $x_i$  are the estimates of the input variables;  $u_c(y)$  is the combined standard uncertainty associated to the output variable  $y$ ; and  $f$  is the function that correlates input variables  $x_i$  to output variable  $y$ .

The standard uncertainty of each measurement is calculated considering its uncertainty and resolution intervals, yielding its type B uncertainty. A rectangular (or uniform) distribution of possible values in these intervals is considered.<sup>3</sup>

The uncertainty of absolute humidity is calculated through Eq. (1). Uncertainty of precipitable water in turn is computed through Eq. (2).

A function that correlates atmospheric transmittance to the amount of precipitable water is obtained from regression of the data in Passman and Larmore tables. The uncertainty of the transmittance is calculated by applying the law of propagation of uncertainty, Eq. (6), to this function.

The power received by the thermal imager is estimated through Eqs. (3) and (5). The power from the inspected

**Table 1** Adopted values for simulations.

Atmospheric temperature	Ambient temperature	Relative humidity	Emissivity of the object	Distance	Temperature of the object
23°C	23°C	50%	0.90	50 m	60°C, 90°C

object is calculated from Eq. (4).<sup>1,25</sup> The uncertainty of the power from the object is estimated by propagating the uncertainty of the transmittance through Eq. (4) and by propagating the uncertainty of emissivity through Eq. (3).

The temperature uncertainty is estimated from the power from the inspected object and its uncertainty through Eqs. (3) and (5). Finally, the thermal imager’s uncertainty should be associated to this result by Eq. (6).

**2.3 Contribution from Each Source to Temperature Measurement Uncertainty**

The calculation of the contribution from each source of uncertainty to the measuring temperature uncertainty by thermography is carried out using the method available in Ref. 29, which is shown in Eq. (7). It should be remembered that the sources of uncertainty of interest are relative humidity, atmospheric temperature, propagation distance, surface emissivity of the inspected object, and the thermal imager.

$$h(T, x_i) = \left[ \frac{c_i \cdot u(x_i)}{u(T)} \right] \cdot [\text{co}(T, x_i)], \tag{7}$$

where  $h(T, x_i)$  is the Kessel coefficient of contribution of the uncertainty of input variable  $u(x_i)$  to the uncertainty

**Table 2** Ranges of standard uncertainties of the inputs adopted for simulations.

Input variable	Range of standard uncertainty
Atmospheric temperature	0 to 2°C
Temperature of objects in the ambient	0 to 2°C
Relative humidity	0 to 5%
Emissivity of the inspected object	0.00 to 0.03
Distance	0.0 to 0.1 m
Thermal imager	1°C, 2°C

of the output variable  $u(T)$  (dimensionless);  $c_i$  is the partial derivate of the function  $T$  with respect to input variable  $x_i$ ; and  $\text{co}(T, x_i)$  is the coefficient of correlation between the output variable  $T$  and the input variable  $x_i$ .

The coefficient of correlation  $\text{co}$  can be calculated according to Eq. (8):<sup>29</sup>

$$\text{co}(T, x_i) = \sum_{j=1}^n \left[ \frac{c_j \cdot u(x_j)}{u(T)} \right] \cdot [\text{co}(x_i, x_j)]. \tag{8}$$

**3 Results**

To evaluate the quality of the results of the uncertainty calculation method proposed in this paper, a comparison is made with the adopted input parameters and the obtained output results available in Refs. 10 and 11.

In these works, the authors had access to the function that relates the radiation received by the thermal imager to the temperature of the inspected object. They also had access to the calculation model of atmospheric transmittance adopted by the manufacturer of the thermal imager. As the method presented here does not consider any model reserved by camera manufacturers, it is expected that the results are similar in magnitude but not exactly the same.

In order to compare our results to the ones available in Ref. 10, the values adopted for the input data in the simulation are listed in Table 1.

To evaluate the influence of the uncertainty of each input data in the uncertainty of the output, and to compare them to results shown in Ref. 10, the variation ranges of input uncertainty presented in Table 2 were adopted.

The results of the sensitivity tests of the standard uncertainty of the temperature measured from the standard uncertainty of the input variables are shown in Figs. 2, 3, 4, 5, and 6.

Next, we assess the contribution of each source of uncertainty to the final uncertainty of the temperature measurement considering the typical characteristics of the measurements performed by the thermographer. These characteristics are shown in Table 3 and were taken from catalogs of instruments commonly used in thermography. The standard uncertainty of each measurement is calculated

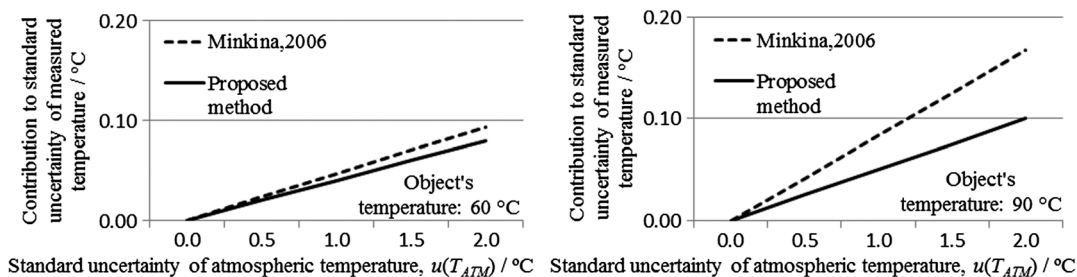


**Fig. 2** Contribution from uncertainty of atmospheric temperature.

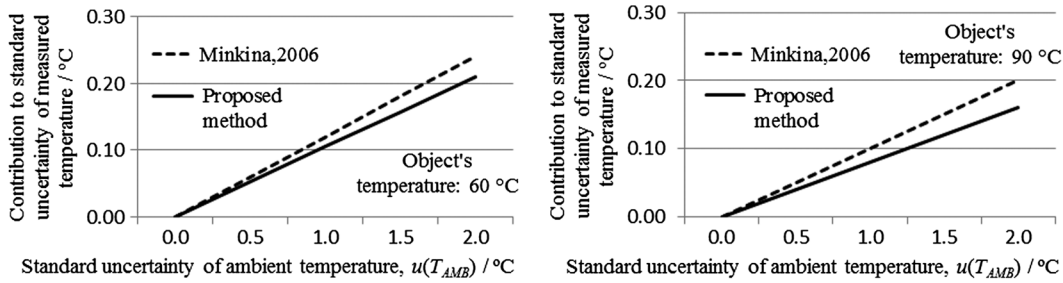


Fig. 3 Contribution from uncertainty of ambient temperature.

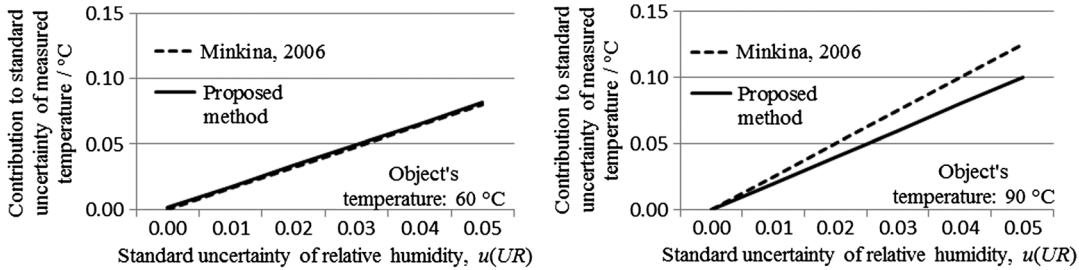


Fig. 4 Contribution from uncertainty of relative humidity.

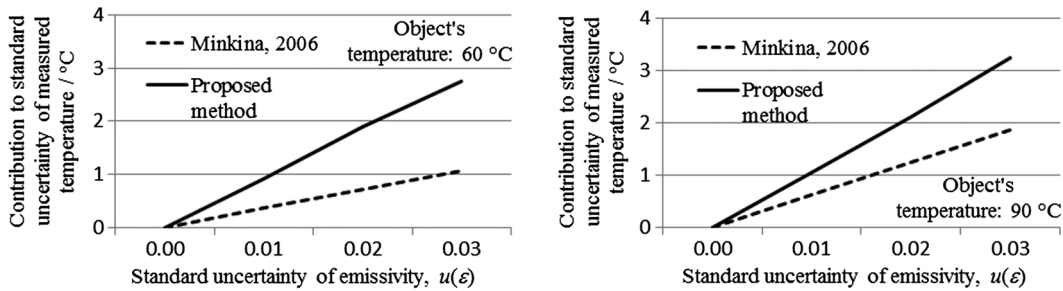


Fig. 5 Contribution from uncertainty of emissivity.

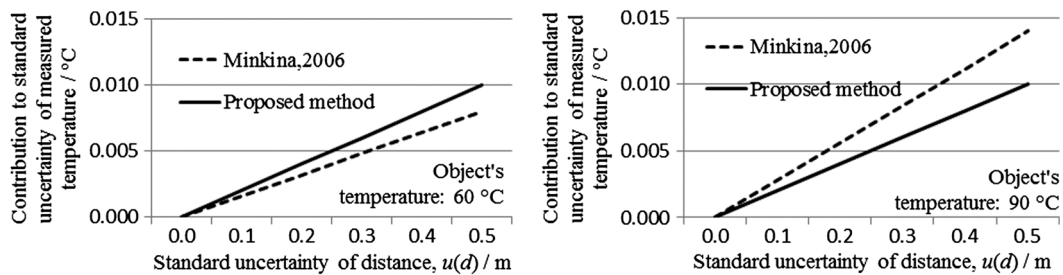


Fig. 6 Contribution from uncertainty of distance.

considering its uncertainty and resolution intervals, yielding its type B uncertainty. A rectangular (or uniform) distribution of possible values in these intervals<sup>3</sup> was considered. The input values adopted were the same as shown in Table 1, considering 60°C for the temperature of the object. The adopted standard uncertainty of emissivity values evaluated by the thermographer is 0.0015 or 0.030. These standard uncertainty of emissivity values are in accordance with expected uncertainty of emissivities close to the unity, between 1 and 4% of emissivity.<sup>30,31</sup>

The results are shown in Tables 4 and 5.

This calculation procedure was compiled in MATLAB 2011b®, producing the output data (variables listed in Table 4) from the instrument characteristics informed by the user (variables listed in Table 3).

Comparison between our results and the results presented in Ref. 11 are presented in Table 6. The values adopted for the simulation are<sup>11</sup> atmospheric and ambient temperatures 20°C; emissivity 0.8; relative humidity 50%; distance 50 m; and object's temperature 90°C.

**Table 3** Instruments used and measurements performed by the thermographer.

Measurement (instrument)	Resolution	Uncertainty range
Atmospheric temperature (thermometer) <sup>32</sup>	0.1°C	1°C
Ambient temperature (thermometer) <sup>33</sup>	0.1°C	1°C
Relative humidity (hygrometer) <sup>32</sup>	1%	5%
Distance (electronic measurement tape) <sup>34</sup>	0.001 m	0.01 m
Radiometric sensitivity (thermal imager) <sup>35,36</sup>	0.1°C	1°C, 2°C

**Table 4** Contribution from each measurement at 0.015 standard uncertainty of emissivity.

Measurement (instrument)	1°C uncertainty thermal imager	2°C uncertainty thermal imager
Atmospheric temperature (thermometer)	<1%	<1%
Ambient temperature (thermometer)	<1%	<1%
Relative humidity (hygrometer)	<1%	<1%
Distance (electronic measurement tape)	<1%	<1%
Radiometric sensibility (thermal imager)	13%	36%
Emissivity (user evaluation)	86%	62%
Measured temperature standard uncertainty	1.6°C	1.9°C

#### 4 Discussion

The results of the sensitivity tests for the uncertainty of the measured temperature by propagation from uncertainties of the input data (Figs. 2, 3, 4, 5, and 6), shown in Sec. 3, demonstrate that the method proposed in this paper provides results close to those shown in Ref. 10. They are developed

**Table 5** Contribution from each measurement at 0.030 standard uncertainty of emissivity.

Measurement (instrument)	1°C uncertainty thermal imager	2°C uncertainty thermal imager
Atmospheric temperature (thermometer)	<1%	<1%
Ambient temperature (thermometer)	<1%	<1%
Relative humidity (hygrometer)	<1%	<1%
Distance (electronic measurement tape)	<1%	<1%
Radiometric sensibility (thermal imager)	4%	15%
Emissivity (user evaluation)	95%	85%
Measured temperature standard uncertainty	2.8°C	3.0°C

**Table 6** Comparison of results for emissivity and ambient temperature uncertainties.

Standard uncertainty of emissivity	Contribution to standard uncertainty of measured temperature	
	Proposed method	Method presented in Ref. 11
0.02	2.5°C	2.5°C
0.03	3.8°C	3.9°C
0.04	5.0°C	4.9°C

from phenomenological and empirical models available to the customer and are similar to those developed from models reserved by manufacturers of thermal imagers and not available. Furthermore, the comparisons made to the work presented in Ref. 11 show very similar results for contributions from emissivity uncertainty.

A discrepancy can be seen between the results for the uncertainty of emissivity of the inspected object when compared to the work presented in Ref. 10, despite being of the same order of magnitude. However, this result is in line with results presented in Ref. 11. As the calculation models used in Ref. 10 are not available, we are not able to discuss this difference.

Sensitivity analysis also shows that the influence of distance, atmospheric and ambient temperatures, and relative humidity measurements is very low in comparison to the influence of the measurement of the emissivity of the inspected object. In fact, the results of the contribution from such sources shown in Tables 4 and 5 seem irrelevant to the uncertainty of the measurement temperature by thermography, under the specified conditions. Emissivity measurement and the intrinsic uncertainty of the thermal imager are the two major factors in the total uncertainty.

From Tables 4 and 5, it can be seen that an increase in the standard uncertainty of emissivity from 0.015 to 0.030 nearly doubles the standard uncertainty of the measured temperature from 1.6 to 2.8°C if the imager has 1°C uncertainty. Less impactful but still significant, a thermal imager with 2°C uncertainty compared to a 1°C uncertainty thermal imager increases the uncertainty of the final result from 1.6 to 1.9°C, by ~19%, if the emissivity standard uncertainty is 0.015.

#### 5 Conclusion

The alternative calculation method of uncertainty of temperature measurement by infrared thermography presented in this work showed results in line with those available in the literature. The proposed method can be used to give an indication of the quality of the temperature measurement performed from an estimate of its uncertainty for diagnosis of the equipment under inspection.

Sensitivity analysis of the uncertainty of the temperature measurement from the uncertainties of the input data showed that of all sources considered, the uncertainties of emissivity and of the thermal imager are the most important factors. Emissivity, which is usually not measured but estimated by the thermographer according to data available in the literature, is the factor with the greatest impact. Therefore, the use

of a thermal imager with low uncertainty and the careful and thoughtful evaluation of emissivity will lead to temperature measurements of a better quality, i.e., with lower uncertainty.

The results indicate that under normal conditions the standard uncertainty of the temperature measured can vary from  $\sim 1.6$  to  $3.0^\circ\text{C}$ . Therefore, the use of a thermal imager with a high level of uncertainty ( $2^\circ\text{C}$ ) or high standard uncertainty of emissivity (0.03), which yields a standard uncertainty of the measured temperature in the range of  $1.9$  to  $3.0^\circ\text{C}$  in established conditions, may lead to misdiagnosis. The acceptance criterion is  $\sim 5^\circ\text{C}$  in predictive maintenance.

As estimating the uncertainty of temperature measurement is shown here to be practicable, and in compliance with technical recommendations,<sup>3</sup> manufacturers of thermal imagers and software developers should provide this function for users.

## References

1. M. Vollmer and K.-P. Möllmann, *Infrared Thermal Imaging*, Wiley-VCH, Weinheim (2010).
2. K. Chrzanowski, *Non-Contact Thermometry: Measurement Errors*, Polish Chapter of SPIE, Warsaw (2001).
3. Bureau International des Poids et Mesures et al., "Evaluation of measurement data—guide to the expression of uncertainty in measurement," JCGM (100:2008) (1st edition 2008, corrected version 2010).
4. K. Chrzanowski, J. Fischer, and R. Matyszkiewicz, "Testing and evaluation of thermal cameras for absolute temperature measurement," *Opt. Eng.* **39**(9), 2535–2544 (2000).
5. Instituto Nacional de Metrologia Qualidade e Tecnologia, "International vocabulary of metrology: basic and general concepts and associated terms," JCGM 200:2012.
6. G. Grđić and I. Pušnik, "Analysis of thermal imagers," *Int. J. Thermophys.* **32**(1–2), 237–247 (2011).
7. K. Chrzanowski and R. Matyszkiewicz, "Software package for uncertainty calculations of temperature measurements with thermal cameras," in *Quantitative Infrared Thermography Conference*, Reims, pp. 97–102 (2000), <http://qirt.gel.ulaval.ca/archives/qirt2000/papers/055.pdf>.
8. K. Chrzanowski et al., "Uncertainty of temperature measurement with thermal cameras," *Opt. Eng.* **40**(6), 1106–1114 (2001).
9. W. Minkina and S. Dudzik, *Infrared Thermography: Errors and Uncertainties*, 1st ed., Wiley, Noida (2009).
10. W. Minkina and S. Dudzik, "Simulation analysis of uncertainty of infrared camera measurement and processing path," *Measurement* **39**(8), 758–763 (2006).
11. B. Lane et al., "Uncertainty of temperature measurements by infrared thermography for metal cutting applications," *Metrologia* **50**(6), 637–653 (2013).
12. M. S. Jadin and S. Taib, "Recent progress in diagnosing the reliability of electrical equipment by using infrared thermography," *Infrared Phys. Technol.* **55**(4), 236–245 (2012).
13. B. R. Lyon, Jr., G. L. Orlove, and D. L. Peters, "The relationship between current load and temperature for quasi-steady state and transient conditions," *Proc. SPIE* **4020**, 62–70 (2000).
14. American National Standards Institute, "ANSI/NETA MTS-2011 standard for maintenance testing specifications for electrical power equipment and systems," (2011).
15. FLIR Systems, User's Manual FLIR InfraCAM SD, 2008, <http://www.alpine-components.co.uk/files/manuals-downloads/FLIR-InfraCAM-SD-Manual.pdf> (16 June 2014).
16. Association for the Advancement of Medical Instrumentation, "ANSI/AAMI DF80—medical electrical equipment," (2010).
17. N. D. S. F. Duarte, Jr., "Management system of measurement: important, but not always recognized," *Metrol. Instrumentação* **7**(56) (2008) (in Portuguese).
18. FLIR Systems Inc., "FLIR customer support center," 27 September 2013, <http://flir.custhelp.com/> (26 June 2013).
19. Fluke Corporation., "Fluke thermal imagers," 09 June 2014, <http://www.fluke.com/fluke/usen/products/categoryti.htm> (11 June 2013).
20. A. G. Testo, "Measuring instruments for the maintenance of electrical installations," 23 April 2013, [http://www.testo.us/en/home/products/thermography/maintenance/electrical\\_maintenance/electrical\\_maintenance.jsp](http://www.testo.us/en/home/products/thermography/maintenance/electrical_maintenance/electrical_maintenance.jsp), (26 June 2014).
21. InfraRed Integrated Systems Ltd., "Thermal cameras—thermography products," July 2010, <http://www.irisys.co.uk/thermal-imaging/products/> (11 June 2013).
22. G. Gaussorgues, *Infrared Thermography*, 3rd ed., Chapman & Hall, London (1994).
23. S. Passman and L. Larmore, *Atmospheric Transmission*, The RAND Corporation, Santa Monica (1956).
24. V. R. Stull, P. J. Wyatt, and G. N. Plass, *The Infrared Absorption of Carbon Dioxide*, Ford Motor Company, New Port Beach (1963).
25. R. Sabatini and M. A. Richardson, *Airborne Laser Systems Testing and Analysis*, North Atlantic Treaty Organisation, Virginia (2010).
26. D. J. C. Coura, "Analysis of the major effects of the propagation of optical signals in free space, coated with a numerical efficient platform," MS Thesis, INATEL, Santa Rita do Sapucaí (2004).
27. P. J. Wyatt, V. R. Stull, and G. N. Plass, "The infrared absorption of water vapor," 1962, <http://www.dtic.mil/dtic/tr/fulltext/u2/297458.pdf> (17 May 2013).
28. F. J. M. Meca, F. J. R. Sanchez, and P. M. Sanchez, "Calculation and optimisation of the maximum uncertainty in infrared temperature measurements taken in conditions of high uncertainty in the emissivity and environment radiation values," *Infrared Phys. Technol.* **43**(6), 367–375 (2002).
29. R. Kessel, R. Kacker, and M. Berglund, "Coefficient of contribution to the combined standard uncertainty," *Metrologia* **43**(4), S189–S195 (2006).
30. J. Ishii and A. Ono, "Uncertainty estimation for emissivity measurements near room temperature with a Fourier transform spectrometer," *Meas. Sci. Technol.* **12**(12), 2103–2112 (2001).
31. M. R. Miller, G. Mulholland, and C. Anderson, "Experimental cutting tool temperature distributions," *J. Manuf. Sci. Eng.* **125**(4), 667 (2003).
32. Minipa, "MT-240 thermohygrometers," 28 January 2014, <http://www.minipa.com.br/5/21/159-Minipa-Termo-higrometros-MT-240> (28 March 2014).
33. Fluke Corporation, "56X infrared thermometer," December 2010, [http://media.fluke.com/documents/56x\\_gseng0000.pdf](http://media.fluke.com/documents/56x_gseng0000.pdf) (28 March 2014).
34. Fluke Corporation, "Fluke 424D, 419D and 414D laser distance meters," April 2012, [http://media.fluke.com/documents/3028711\\_0000\\_ENG\\_E\\_W.PDF](http://media.fluke.com/documents/3028711_0000_ENG_E_W.PDF) (28 March 2014).
35. FLIR Systems Inc, "FLIR® ex-series infrared camera specifications," 2013, <http://www.flir.com/thermography/americas/us/view/?id=61194&collectionid=830&col=61196> (28 March 2014).
36. FLIR, "Technical data FLIR P660," 27 May 2014, [http://support.flir.com/DsDownload/Assets/40402-3001\\_en\\_50.pdf](http://support.flir.com/DsDownload/Assets/40402-3001_en_50.pdf) (07 May 2014).

**Pablo Rodrigues Muniz** received his BSc and MSc degrees in electrical engineering and mechanical engineering, respectively, from the Universidade Federal do Espírito Santo, Brazil, in 2002 and 2006, respectively. He is currently working toward his Dr. degree at Universidade Federal da Bahia, Salvador, BA, Brazil. He is with Instituto Federal do Espírito Santo, Vitória, ES, Brazil, as a professor. He had worked as maintenance specialist at electrical shop and engineering division at ArcelorMittal Tubarão.

**Ricardo de Araújo Kalid** received his BSc and MSc degrees from Universidade Federal da Bahia in 1988 and 1991, respectively, and received his PhD degree in 1999 from Universidade de São Paulo, all in chemical engineering. He has experience in industrial and chemical engineering. He coordinates several research efforts concerning industrial processes. He is currently professor at Universidade Federal da Bahia and dean *Pro Tempore* of Universidade Federal do Sul da Bahia.

**Shirley P. N. Cani** received her BSc, MSc, and PhD degrees, all in electrical engineering, from the Universidade Federal do Espírito Santo, Vitória, Brazil, in 2001, 2003, and 2007, respectively. During her MSc and PhD studies, she was involved in optical communication research. Since 2008, she has been with the Electrotechnical Department, Instituto Federal do Espírito Santo.

**Robson da Silva Magalhães** received his BSc, MSc, and DSc degrees in mechanical engineering, electrical engineering, and industrial engineering, respectively, from the Universidade Federal da Bahia, Salvador, Brazil, in 1985, 2005, and 2010, respectively. He has experience in industrial maintenance, emphasizing on vibration and motor current signature analysis. He is currently a professor with the Chemical Engineering Department, Universidade Federal da Bahia.